



Differential effects of nitrogen vs. phosphorus limitation on terrestrial carbon storage in two subtropical forests: A Bayesian approach

Zhenggang Du^a, Jiawei Wang^a, Guiyao Zhou^a, Shahla Hosseini Bai^b, Lingyan Zhou^a, Yuling Fu^a, Chuankuan Wang^c, Huiming Wang^d, Guirui Yu^d, Xuhui Zhou^{a,*}

^a Tiantong National Field Observation Station for Forest Ecosystem, Center for Global Change and Ecological Forecasting, School of Ecological and Environmental Sciences, East China Normal University, Shanghai 200062, China

^b Centre for Planetary Health and Food Security, School of Environment and Science, Griffith University, Nathan, QLD 4111, Australia

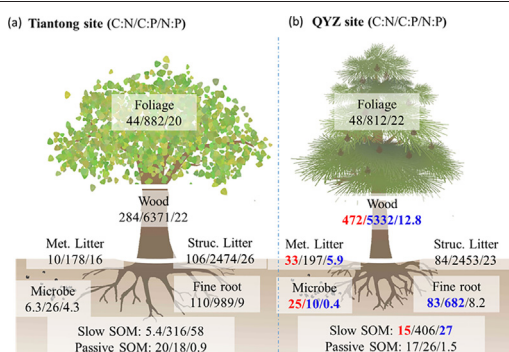
^c Center for Ecological Research, Northeast Forestry University, Harbin 150040, China

^d Institute of Geographical Sciences and Natural Resource Research, Chinese Academy of Sciences, Beijing 100101, China

HIGHLIGHTS

- Effects of N and P limitation on C cycle were different in two subtropical forests.
- Stoichiometry of wood biomass and soil microbe was good indicator of N/P limitation
- Bayesian approach is suitable to evaluate effect of imbalanced nutrient limitation

GRAPHICAL ABSTRACT



ARTICLE INFO

Article history:

Received 2 February 2021

Received in revised form 11 June 2021

Accepted 12 June 2021

Available online 24 June 2021

Editor: Fang Wang

Keywords:

Nutrient limitation

Nitrogen process

Phosphorus process

Data assimilation

Biological stoichiometry

ABSTRACT

Nitrogen (N) and phosphorus (P) have been demonstrated to limit terrestrial carbon (C) storage in terrestrial ecosystems. However, the reliable indicator to infer N and P limitation are still lacking, especially in subtropical forests. Here we used a terrestrial ecosystem (TECO) model framework in combination with a Bayesian approach to evaluate effects of nutrient limitation from added N/P processes and data sets on C storage capacities in two subtropical forests (Tiantong and Qianyanzhou [QYZ]). Three of the six simulation experiments were developed with assimilating data (TECO C model with C data [C-C], TECO C-N coupling model with C and N data [CN-CN], and TECO C-N-P model with C, N, and P data [CNP-CNP]), and the other three ones were simulated without assimilating data (C-only, CN-only, and CNP-only). We found that P dominantly constrained C storage capacities in Tiantong (42%) whereas N limitation decreased C storage projections in QYZ (44%). Our analysis indicated that the stoichiometry of wood biomass and soil microbe (e.g., N:P ratio) were more sensitive indicators of N or P limitation than that of other pools. Furthermore, effects of P-induced limitation were mainly on root biomass by additional P data and on both metabolic litter and soil organic carbon (SOC) by added P processes. N-induced effects were mainly from added N data that limited plant non-photosynthetic tissues (e.g., woody biomass and litter). The different effects of N and P modules on C storage projections reflected the diverse nutrient acquisition strategies associated with stand ages and plant species under nutrient stressed environment. These findings suggest that the interaction between plants and microorganisms regulate effects of nutrient availability on ecosystem C storage, and stoichiometric flexibility of N and P in plant and soil C pools could improve the representation of N and P limitation in terrestrial ecosystem models.

© 2021 Elsevier B.V. All rights reserved.

* Corresponding author at: School of Ecological and Environmental Sciences, East China Normal University, 500 Dongchuan Road, Shanghai 200062, China.
E-mail address: xhzhou@des.ecnu.edu.cn (X. Zhou).

1. Introduction

The availability of macronutrients, predominantly nitrogen (N) and phosphorus (P), widely constrains the fluxes and storage of carbon (C) in terrestrial ecosystems. These nutrients are the most elusive factors in predicting the size of the terrestrial sink and the future climate-C cycle feedback (Vitousek and Howarth, 1991; Hungate et al., 2003; Arora et al., 2013). As atmospheric CO₂ concentration increases, plants will require great soil mineral nutrients to facilitate the enhanced photosynthesis and tissue construction (Finzi et al., 2006; Melillo et al., 2011; Norby et al., 2010). On the other hand, the enhanced C assimilation will dilute tissue nutrient concentration and decrease litter quality (i.e., higher litter C:N:C:P ratio; Craine et al., 2009; Kou-Giesbrecht and Menge, 2019; Vigulu et al., 2019). Meanwhile, soil microbes decomposing the low-quality litter may need to immobilize more nutrients to maintain their stoichiometric balance, which further exacerbates nutrient limitations (Luo et al., 2004, 2006; Reich et al., 2006). Increased external nutrient inputs (e.g., N deposition, parent material weathering) and accelerated nutrient mineralization rates under climatic warming may enhance soil nutrient availability (Melillo et al., 2002) and partly alleviate plant-microbe nutrient competition (Hungate et al., 2003; Wieder et al., 2015b). However, whether these additional nutrients are sufficient to meet the enhanced plant nutrient demands in natural ecosystems remains unknown.

Generally, temperate and boreal ecosystems are N-limited due to slow N mineralization, while tropical forests and savannah ecosystems are P-limited in their highly weathered soil (Cleveland et al., 2002; Lebauer and Treseder, 2008; Li et al., 2016). These phenomena have been largely confirmed by field manipulative experiments with elevated CO₂ and/or nutrient addition (i.e., N and P fertilization) (Norby et al., 2010; Reich et al., 2006; Tian et al., 2019), which have yielded valuable insight into our understanding of nutrient limitation on terrestrial C cycling (Liu et al., 2013; Niu et al., 2016; Zheng et al., 2019). However, previous studies are most based on manipulative experiments in which the potential consequences of perturbation (i.e., N and P addition) are largely intertwined. Thus, the magnitudes of nutrient limitation effects on natural ecosystems and their interactions with the climate system are less quantified (Vitousek and Howarth, 1991; Galloway et al., 2004; Armeth et al., 2010).

Nitrogen deposition has increased dramatically in recent decades through human-caused reactive N input (Jia et al., 2014; Bai et al., 2015). It is expected that subtropical forests will respond differently to increasing N deposition due to indirect effects of P and cation availability (Liu et al., 2013; Fan et al., 2015; Zheng et al., 2015). However, the only source of atmospheric P deposition is through dust and flying ash from wildfires, which is relatively small in amount and difficult for plants to directly assimilate (Mahowald et al., 2008; Peñuelas et al., 2012, 2013). Thus, the imbalanced N and P inputs into the subtropical forest ecosystems would drive the nutrient availability toward more P limitation (Li et al., 2016; Q. Zhang et al., 2017; X. Zhang et al., 2017; Jiang et al., 2018). It is still not well characterized that how much N and/or P limits plant biomass and production as well as ecosystem C storage in subtropical ecosystems.

Terrestrial ecosystem models can be used to predict the land C storage dynamic and its feedback to climate but with large uncertainties (Friedlingstein et al., 2006; Ahlström et al., 2012; Arora et al., 2013). One of the major sources of uncertainty is how to accurately represent effects of N and/or P limitation on biogeochemical models (Hungate et al., 2003; Wieder et al., 2015b; Thomas et al., 2015). Most terrestrial models typically implement a fixed or narrow flexible stoichiometric relationship between C and N/P among different pools to maintain the internal stoichiometry between nutrient external supply and assimilation by organisms (Thornton et al., 2009; Wang et al., 2010; Zaehle and Friend, 2010). The effects of nutrient limitation on plant growth or NPP might thus occur if the nutrient supply cannot keep up demand of tissue construction (Thomas et al., 2015; Averill and Waring, 2018; Du et al.,

2018; Omidvar et al., 2021). However, model representation of the fixed or narrow flexible ratios of elements among different pools has made it difficult to capture effects of imbalanced N and P inputs on C storage capacities under different nutrient stressed environment. Furthermore, only a few ecosystem models or land surface models represent C-N-P biogeochemistry (e.g., CABLE and DNDC; Wang et al., 2010; Gilhespy et al., 2014; Zhu et al., 2019), which have proven more complicated to quantify the uncertainties arising from those additional N and P processes (Wieder et al., 2015a; Du et al., 2017; Shi et al., 2018).

This study was designed to address the hypothesis that the flexible stoichiometries (i.e., C:N:P ratios) of plants and soil are sensitive indicators of soil nutrient availability in different nutrient stressed environments. We further hypothesize that added N and P module may differentially limit model projection of ecosystem C storage in N- and P-limited forests. Six experiments were conducted to distinguish the information from N/P modules in constraining key parameters (C turnover rate, C:N, C:P ratios and C allocation rate) in two subtropical forest ecosystems by model intercomparisons in a terrestrial ecosystem (TECO) model framework with Bayesian approach. The Shannon information index (SII) was used to calculate the relative information gains from both the N and P modules (including processes, measurements, and both), using a random variable as represented by probabilistic density functions (Weng and Luo, 2011; Du et al., 2017).

2. Materials and methods

2.1. Site information and data source

The data used in this study were obtained from two subtropical forest ecosystem sites, both of which have been described in Zhang et al. (2010), Du et al. (2015), H. Liu et al. (2019) and R. Liu et al. (2019). In brief, the Tiantong site (Tiantong) is situated in a subtropical evergreen broad-leaved plantation in Zhejiang Province, China (29°48' N, 121°47' E). This area is characterized as a subtropical monsoon climate with humid hot summers and dry cold winters (Zhou et al., 2017). Mean annual temperature is 16.2 °C, ranging from 4.2 °C in January to 28.2 °C in July and mean annual precipitation is 1374 mm, which mainly occurs from May to August (data from China Climatological Survey in Tiantong, Zhejiang). The soil type is Acrisol with texture is mainly sandy to silty clay loam, and pH ranges from 4.4 to 5.1 (Yan et al., 2006). The dominant tree species in this region include *Castanopsis fargesii*, *Lithocarpus glaber* and *Schima superba*, and the age of the plantations is about 60 years old (H. Liu et al., 2019; R. Liu et al., 2019). The N and P depositions of this region are 36.02 kg N ha/y and 0.75 kg P ha/y, respectively (Zhu et al., 2016).

Qianyanzhou site (QYZ) is located in Jiangxi Province, China (26°44' N, 115°03' E) and is a subtropical evergreen coniferous plantation, established in 1980s on a former evergreen broadleaf forest (Huang et al., 2007). The dominant species of current vegetation are *Pinus massoniana*, *P. elliotii* and *Cunninghamia lanceolata*. By 2017, the age of the three plantations was approximately 32 years old (Dai et al., 2018). Based on the meteorological records from 1985 to 2007, the mean annual temperature and precipitation were 17.9 °C and 1475 mm, respectively (Wen et al., 2010). Soils weathered from red sandstone and mudstone are classified as Typic Dystrudepts, Udepts and Inceptisols (Wang et al., 2012), and pH ranges from 4.5 to 5.2 (Mo et al., 2018). The N and P depositions of this region is about 18.4 kg N ha/y and 0.74 kg P ha/y, respectively (Zhu et al., 2016; Gao et al., 2017).

Data used in this study included climatic and biotic variables, including air temperature at top canopy [Ta], photosynthetically active radiation [PAR], relative humidity [RH], leaf area index [LAI], and C-related measurements in the corresponding N and P data sets. The C-related measurements included foliage, woody and fine root biomass, litterfall, microbial C, forest floor C, soil C, soil respiration and LAI. The corresponding N and P data sets included N and P pools in foliage, woody tissues, fine roots, microbes, forest floor, and mineral soil, litterfall N and P, soil inorganic N and P, net soil N and P mineralization, plant N and P

uptake, N and P input from atmospheric deposition, and biological N fixation and soil P weathering. The biotic data were described elsewhere, for Tiantong site in Gao et al. (2014), Zheng et al. (2017), K. Zhang et al. (2020) and P. Zhang et al. (2020), and for QYZ site in Li et al. (2006), Zhang (2013), Q. Zhang et al. (2017) and X. Zhang et al. (2017). The measurement methods, times, and frequencies for these data sets have been described in detail by Du et al. (2015, 2017), H. Liu et al. (2019) and R. Liu et al. (2019). At Tiantong site, the climatic variables were available from 1953 to 2010, and the biotic measurements were collected from 2011 to 2015. At QYZ site, the climatic variables were available from 1980 to 2010, and the biotic measurements were collected from 2003 to 2009. The climatic variables of the both sites were downloaded from the Chinese Ecosystem Research Network (CERN, www.cern.ac.cn).

2.2. Model description

Both the Terrestrial Ecosystem C-N coupling model (TECO-CN) and C-N-P coupling model (TECO-CNP) used in this study are variants of the TECO C-only version (TECO-C) incorporating additional key N and P processes, respectively (Fig. 1). The TECO-C model is a process-based ecosystem model designed to examine critical processes regulating interactive responses of plants and ecosystems to climate change (Luo and Reynolds, 1999). Based on the TECO-C model, the TECO-CN has been developed by incorporating C:N ratio with eight various C and N pools in addition to soil mineral N pool (Fig. 1) as extensively described in Shi et al. (2016) and Du et al. (2017). The TECO-CNP follows the TECO-CN approach with some modifications including eight tissue P pools (i.e., foliage, woody, fine roots, metabolic and structural litter, fast, slow and passive soil organic matter) and three soil mineral P pools (i.e., soil labile P, sorbed P and strongly sorbed P).

In the TECO-CNP model, carbon enters the ecosystem via canopy photosynthesis (i.e., GPP) while N and P are assimilated by plants from mineral soil, and are then allocated into foliage biomass (X_1), woody biomass (X_2), and fine roots (X_3). Dead plant materials enter into the metabolic (X_4) and structural litter (X_5) compartments, and are decomposed by microbes (X_6). Part of the litter C is respired, and

the remaining is converted into slow (X_7) and passive SOM (X_8). The N and P transfer follow the same path with C within the ecosystem, and can be expressed mathematically by the following three matrix equations:

$$\begin{cases} \frac{dX}{dt} = BU(t) - \xi(t)ACX(t) \\ \frac{dN}{dt} = r_u N_{min}(t)\Pi - \xi(t)ACR^{-1}X(t) \\ \frac{dP}{dt} = \varepsilon_u P_{lab}(t)\Theta - \xi(t)ACS^{-1}X(t) \\ X(0) = X_0; N(0) = N_0; P(0) = P_0 \end{cases} \quad (1)$$

where $X = (X_1, X_2, \dots, X_8)^T$, $N = (N_1, N_2, N_3, \dots, N_8)^T$ and $P = (P_1, P_2, P_3, \dots, P_8)^T$ are 8×1 vectors, representing sizes of C, N and P in foliage, wood, fine roots, metabolic litter, structural litter, microbes, slow and passive SOM, respectively. $B = (b_1, b_2, b_3, 0, 0, 0, 0, 0)^T$, $\Pi = (\pi_1, \pi_2, 1 - \pi_1 - \pi_2, 0, 0, 0, 0, 0)^T$ and $\Theta = (\theta_1, \theta_2, 1 - \theta_1 - \theta_2, 0, 0, 0, 0, 0)^T$ are vectors of allocation coefficients of C, N and P assimilated into leaves, woody tissues and fine roots, respectively. $U(\cdot)$ is the C input fixed by canopy-level photosynthesis (i.e., gross primary productivity, GPP). r_u and ε_u are the rate of plant N and P uptake, respectively. $N_{min}(\cdot)$ and $P_{lab}(\cdot)$ represent amounts of available N and P in the soil, respectively. $\xi(\cdot)$ is a scaling function accounting for temperature and moisture effects on C decomposition. A and C are 8×8 matrices given by

$$A = \begin{pmatrix} -1 & 0 & 0 & 0 & 0 & 0 & 0 & 0 \\ 0 & -1 & 0 & 0 & 0 & 0 & 0 & 0 \\ 0 & 0 & -1 & 0 & 0 & 0 & 0 & 0 \\ 0.712 & 0 & 0.712 & -1 & 0 & 0 & 0 & 0 \\ 0.288 & 1 & 0.288 & 0 & -1 & 0 & 0 & 0 \\ 0 & 0 & 0 & 0.45 & 0.275 & -1 & 0.42 & 0.45 \\ 0 & 0 & 0 & 0 & 0.275 & 0.296 & -1 & 0 \\ 0 & 0 & 0 & 0 & 0 & 0.004 & 0.03 & -1 \end{pmatrix}; C = \text{diag}(C) \quad (2)$$

where $\text{diag}(C)$ denotes an 8×8 diagonal matrix with diagonal entries given by the vector $c = (c_1, c_2, \dots, c_8)^T$. Components $c_j (j = 1, 2, \dots, 8)$

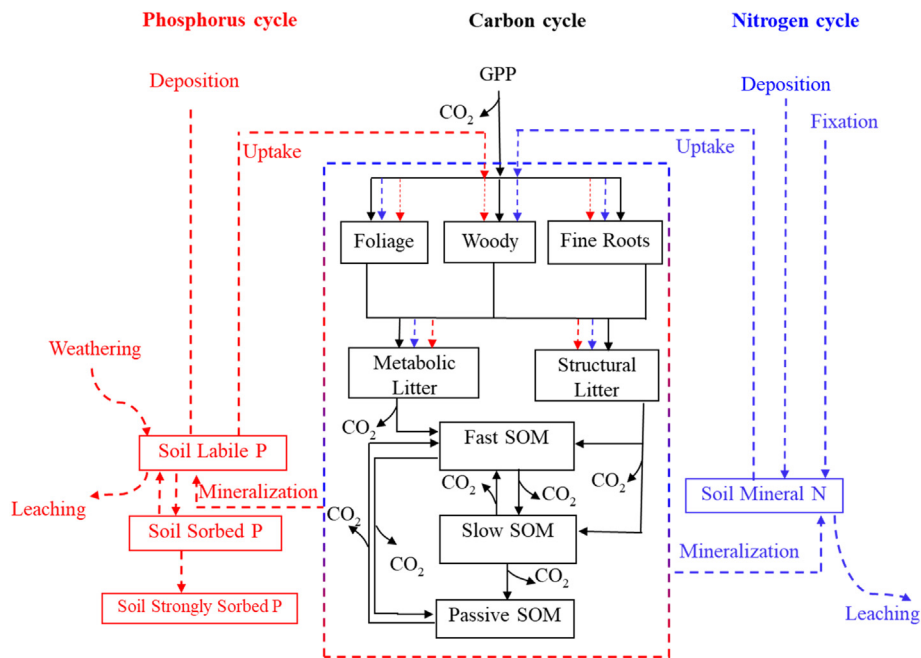


Fig. 1. Schematic diagram of the terrestrial ecosystem carbon (C), nitrogen (N) and phosphorus (P) coupling model (TECO-CNP). Black arrows indicate C-cycle processes, blue arrows show N-cycle processes and red arrows show P-cycle processes. SOM, soil organic matter.

represent C transfer coefficients associated with pool X_j ($j = 1, 2, \dots, 8$). R and S are 8×8 diagonal matrix with the diagonal elements given by the vectors $R = (r_1, r_2, r_3, \dots, r_8)^T$ and $S = (s_1, s_2, s_3, \dots, s_8)^T$, representing the C:N and C:P ratios in the eight organic pools (i.e.), respectively. In this study, the key parameters, including C transfer coefficients, C:N ratio, C:P ratio, and 9 other parameters for calculating nutrient uptake and allocation were estimated simultaneously (Table S1).

2.3. Data assimilation with Bayesian inversion approach

A Bayesian probabilistic inversion approach was employed to identify model parameters by combing models with data. A detailed description of the data assimilation approach was given by Xu et al. (2006), Zhou et al. (2010), and Du et al. (2017) as well as Appendix A. Here, we only provided a brief overview.

To apply Bayes' theorem, we first specified the prior probability density function (PDF) $p(c)$ by giving a set of limiting intervals for parameters c with uniform distribution (Table S1), and then constructed the likelihood function $p(Z|c)$ on the basis of the assumption that observation errors followed a Gaussian distribution. The likelihood function $p(Z|c)$ was specified according to distributions of observation errors ($e_i(t)$).

$$P(Z|c) \propto \exp \left\{ -\sum_i \frac{1}{2\sigma_i^2} \sum_{t \in \text{obs}(Z_i)} (e_i(t))^2 \right\} \quad (3)$$

where σ_i^2 is the measurement error variance of each dataset and $e_i(t)$ is the error for each modeled value $X_i(t)$ compared with the observed value $Z_i(t)$ at time t .

Generally, added modules can improve model ability to capture ecosystem responses to environmental changes but may increase uncertainty with less identifiable parameters. Meanwhile, increasing the observational data sets would decrease the uncertainty to a certain degree by providing additional information. There are two criterions to verify model simulation with Bayesian analysis (Du et al., 2017). One criterion is the posterior PDFs of those estimated parameters, and another criterion to judge the validity is the comparison between simulated and observed data (Wu et al., 2009; Weng and Luo, 2011; Du et al., 2015).

Six data assimilation experiments were conducted as follows: (i) TECO-C model without assimilating data (C-only) and (ii) with assimilating eight sets of C data (i.e., foliage, woody, and fine root biomass, litterfall, forest floor C, microbial C, soil C, and soil respiration, C-C); (iii) TECO-CN model without assimilating data (CN-only) and (iv) with assimilating both C and N data (i.e., N in foliage, woody tissues, fine roots, litter fall, microbes, forest floor, and mineral soil, soil inorganic N, plant N uptake, and external N input, CN-CN); (v) TECO-CNP model without assimilating data (CNP-only) and (vi) with assimilating C, N and P data (i.e., P in foliage, woody tissues, fine roots, litter fall, microbes, forest floor, and mineral soil, soil inorganic P, plant P uptake, and external P input, CNP-CNP).

2.4. Relative changes and information contributions on C pools

Model inter-comparisons were used to calculate the relative changes of C pools (RCP) from nutrient modules. The relative changes from N processes (RCP_i^{NP}), data (RCP_i^{ND}) and both (N module, RCP_i^{NM}) were calculated as

$$\begin{cases} RCP_i^{NM}(t) = \log_2 \frac{X_i^{CN-CN}(t)}{X_i^{C-C}(t)} \\ RCP_i^{NP}(t) = \log_2 \frac{X_i^{CNP}(t)}{X_i^C(t)} \\ RCP_i^{ND}(t) = RCP_i^{NM}(t) - RCP_i^{NP}(t) \end{cases} \quad (4)$$

where $X_i^{CN-CN}(t)$, $X_i^{C-C}(t)$, $X_i^{CNP}(t)$ and $X_i^C(t)$ ($i = 1, 2, \dots, 8$) are the C pool sizes simulated in CN-CN, C-C, CN-only and C-only models at time t , respectively. Similarly, the RCPs from P processes (RCP_i^{PP}), data (RCP_i^{PD}) and both (P module, RCP_i^{PM}) were calculated as:

$$\begin{cases} RCP_i^{PM}(t) = \log_2 \frac{X_i^{CNP-CNP}(t)}{X_i^{CN-CN}(t)} \\ RCP_i^{PP}(t) = \log_2 \frac{X_i^{CNP}(t)}{X_i^{CN}(t)} \\ RCP_i^{PD}(t) = RCP_i^{PM}(t) - RCP_i^{PP}(t) \end{cases} \quad (5)$$

where $X_i^{CNP-CNP}(t)$ and $X_i^{CNP}(t)$ ($i = 1, 2, \dots, 8$) are the C pool sizes simulated in CNP-CNP and CNP-only models at time t , respectively.

The relative information gains (Kullback and Leibler divergence, D_{KL}) (Kullback and Leibler, 1951) which calculate the differences in the distributions of simulated C pools between two versions of the TECO framework (CN-CN and C-C, CN and C-only, CNP-CNP and CN-CN, CNP and CN-only). The relative information gain (D_{KL}) was calculated as

$$D_{KL}(p(X_{m2})||p(X_{m1})) = \sum_{i=1}^n p(x_{m2,i}) \log_2 \frac{p(x_{m2,i})}{p(x_{m1,i})} \quad (6)$$

3. Results

3.1. Parameter estimation and comparison

In Tiantong site, eight parameters for TECO-C model with C data (C-C), three for TECO C-N coupling model with C and N data (CN-CN), and six for TECO C-N-P model with C, N, and P data (CNP-CNP) relating to the C cycle were well constrained in the three experiments with assimilating observation (Fig. 2a). Seven parameters associated with the N cycle were well constrained in CN-CN and CNP-CNP (Fig. 2b), and seven parameters related to the P cycle were well constrained in CNP-CNP (Fig. 2c). However, in QYZ site, the number of well-constrained parameters with assimilating data had nine parameters for C-C, ten for CN-CN, and nine for CNP-CNP relating to C cycle (Fig. 3a); seven parameters for CN-CN and five for CNP-CNP relating to N cycle (Fig. 3b); and six parameters for CNP-CNP relating to P cycle (Fig. 3c). Without assimilating data, almost all parameters were not constrained (Figs. 2 and 3).

Although these parameters were well constrained when assimilating observational data sets, the estimated median of boxplots of most parameters among experiments were considerably different (Figs. 2 and 3). For these C-related parameters, the medians of C_1 (1.82 mg C $g^{-1} d^{-1}$ for Tiantong and 1.89 mg C $g^{-1} d^{-1}$ for QYZ, respectively), C_6 (13.1 and 5.8 mg C $g^{-1} d^{-1}$), b_1 (0.19 and 0.25 mg C $g^{-1} d^{-1}$) and b_3 (0.38 and 0.4 mg C $g^{-1} d^{-1}$) were highest in C-C, respectively, while the Medians of C_4 (3.7 and 6.6 mg C $g^{-1} d^{-1}$) and C_7 (0.11 and 0.057 mg C $g^{-1} d^{-1}$) in CN-CN, and those of C_2 (0.42 and 1.3 mg C $g^{-1} d^{-1}$), C_5 (1.5 and 1.3 mg C $g^{-1} d^{-1}$), C_8 (0.024 and 0.008 mg C $g^{-1} d^{-1}$) and b_2 (0.36 and 0.47 mg C $g^{-1} d^{-1}$) in CNP-CNP were highest (Figs. 2a and 3a).

For those N-related parameters in Tiantong site, the medians of CN_3 (29.4 mg C $g^{-1} d^{-1}$), CN_6 (1.05 mg C $g^{-1} d^{-1}$), CN_7 (5.40 mg C $g^{-1} d^{-1}$) and CN_8 (4.01 mg C $g^{-1} d^{-1}$) were no significant differences between CN-CN and CNP-CNP, but CN_2 was higher in CNP-CNP (425.7 mg C $g^{-1} d^{-1}$) than that in CN-CN (280.4 mg C $g^{-1} d^{-1}$). However, in the QYZ site, the medians of CN_6 (31.6 mg C $g^{-1} d^{-1}$) and ku (126.3 mg C $g^{-1} d^{-1}$) were higher in CN-CN than in CNP-CNP (24.4 and 26.4 mg C $g^{-1} d^{-1}$, respectively). The medians of CN_1 (46.9 mg C $g^{-1} d^{-1}$), CN_2 (455.9 mg C $g^{-1} d^{-1}$), CN_3 (80.6 mg C $g^{-1} d^{-1}$) and CN_5 (10.5 mg C $g^{-1} d^{-1}$) were higher in CNP-CNP than those in CN-CN.

Compared with those in Tiantong site, a combination of higher C:N ratios and lower C:P ratio led to lower N:P ratios for several C pools in

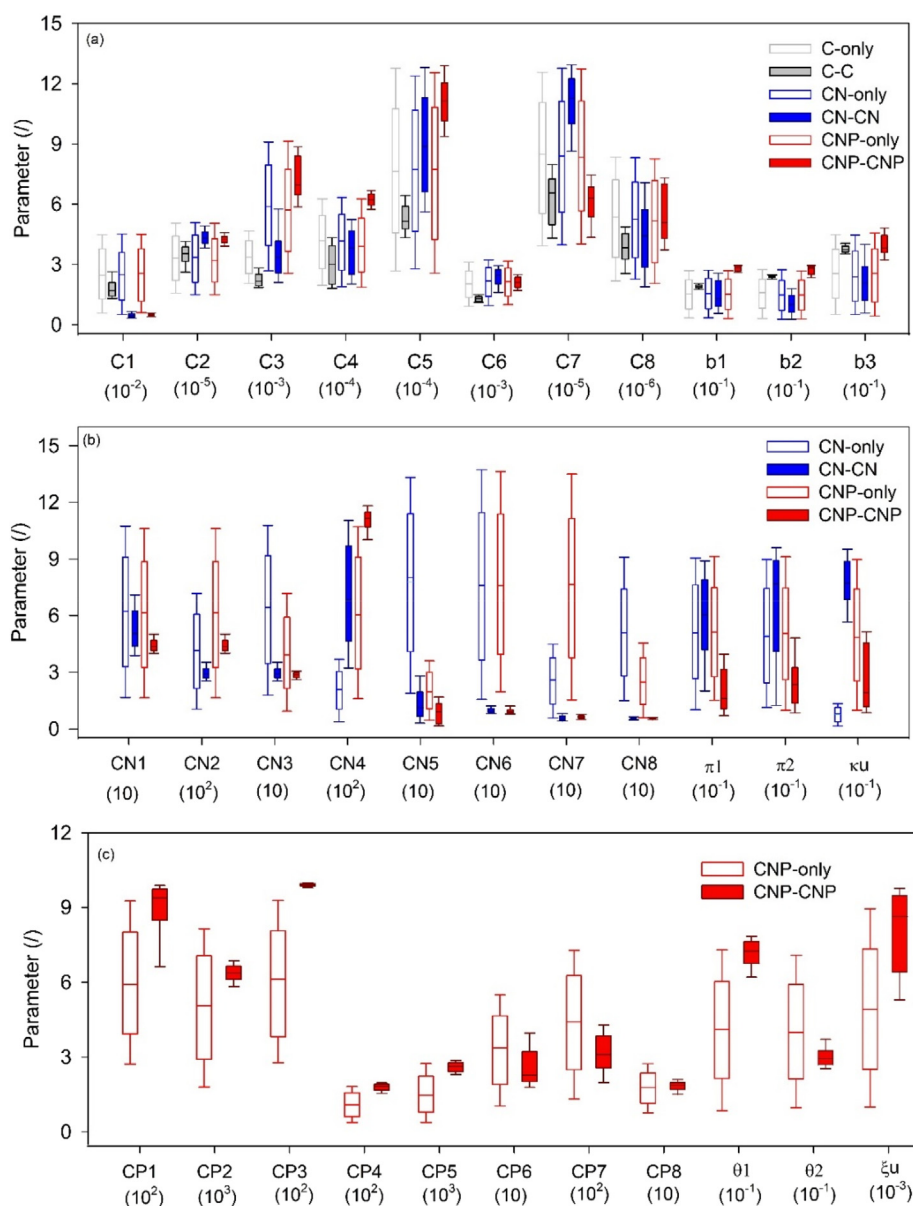


Fig. 2. Median (central line), 25 to 75% range (wide boxes), 5 to 95% range (whiskers) for 11 parameters relating to carbon (C) cycle across all six assimilation experiments (panel a), for 11 parameters relating to nitrogen (N) cycle in four experiments (i.e., CN-only, CN-CN, CNP-only and CNP-CNP, respectively, panel b), and for 11 parameters relating to phosphorus (P) cycle of both the CNP-only and CNP-CNP (panel c) in the Tiantong site. See Table S1 for parameter abbreviations and units.

QYZ site (Fig. 4), such as woody biomass (N:P ratio of 12.8 for QYZ vs. 22 for Tiantong), metabolic litter (5.9 vs. 16) and Microbe (0.4 vs. 4.3) pools. However, the lower N:P ratio (27 vs. 58) for slow SOM pool in QYZ might be mainly caused by the higher C:N ratio (15 vs. 5.4) compared with that in Tiantong site. The stoichiometries (i.e., C:N, C:P and N:P ratios) for the rest of C pools, including foliage, structural litter, and passive SOM, were no significant difference between the two sites.

3.2. C storage forecasts and relative contributions of nutrient modules

In both Tiantong and QYZ sites, long-term forecasts of the C storage increased at first and then slowly reached the plateau for all six experiments (Fig. 5). The annual C storage size varied considerably from 77.7 kg C m⁻² for CNP-CNP experiment to 142.0 kg C m⁻² for C-C in Tiantong site at the end of this century (Fig. 4a), and from 81.4 for CN-only to 132.2 kg C m⁻² for C-C in QYZ site (Fig. 5b). Assimilation of data sets substantially reduced variations of forecasted C contents

among the three experiments except the CN-CN experiment in Tiantong site. Additionally, assimilating nutrient data introduced their limitation effects on C projections for CNP-CNP by 45.3% in Tiantong site, and by 25.6% for CN-CN and 13.4% for CNP-CNP in QYZ site.

The effects of nutrient modules among C pools changed largely between the two sites (Fig. 6). In Tiantong site, most C pools were limited by additional N data, such as wood biomass (X_2 , -148%), metabolic litter (X_4 , -64.5%), structural litter (X_5 , -137%), and fast (X_6 , -152%), slow (X_7 , -144%) and passive (X_8 , -37.3%) SOM, but foliage biomass (X_1 , +142%) and fine root pool (X_3 , +49.4%) increased as well as stimulated effects of added N processes on all C pools except fine root pool (X_2 , -47.3%). Additional P data and processes induced positive (i.e., X_1 [+74.5%], X_2 [+150%], X_5 [+67.9%], X_6 [+123%], X_7 [+190%], X_8 [+71.6%]) and negative (i.e., X_2 [-10.5%], X_3 [-4.8%], X_4 [-239%], X_5 [-114%], X_6 [-254%], X_7 [-180%], X_8 [-155%]) effects for most C pools. However, in the QYZ site, additional N data limited woody biomass (-50.5%), fine root (-12.9%), structural litter (-72.4%), and

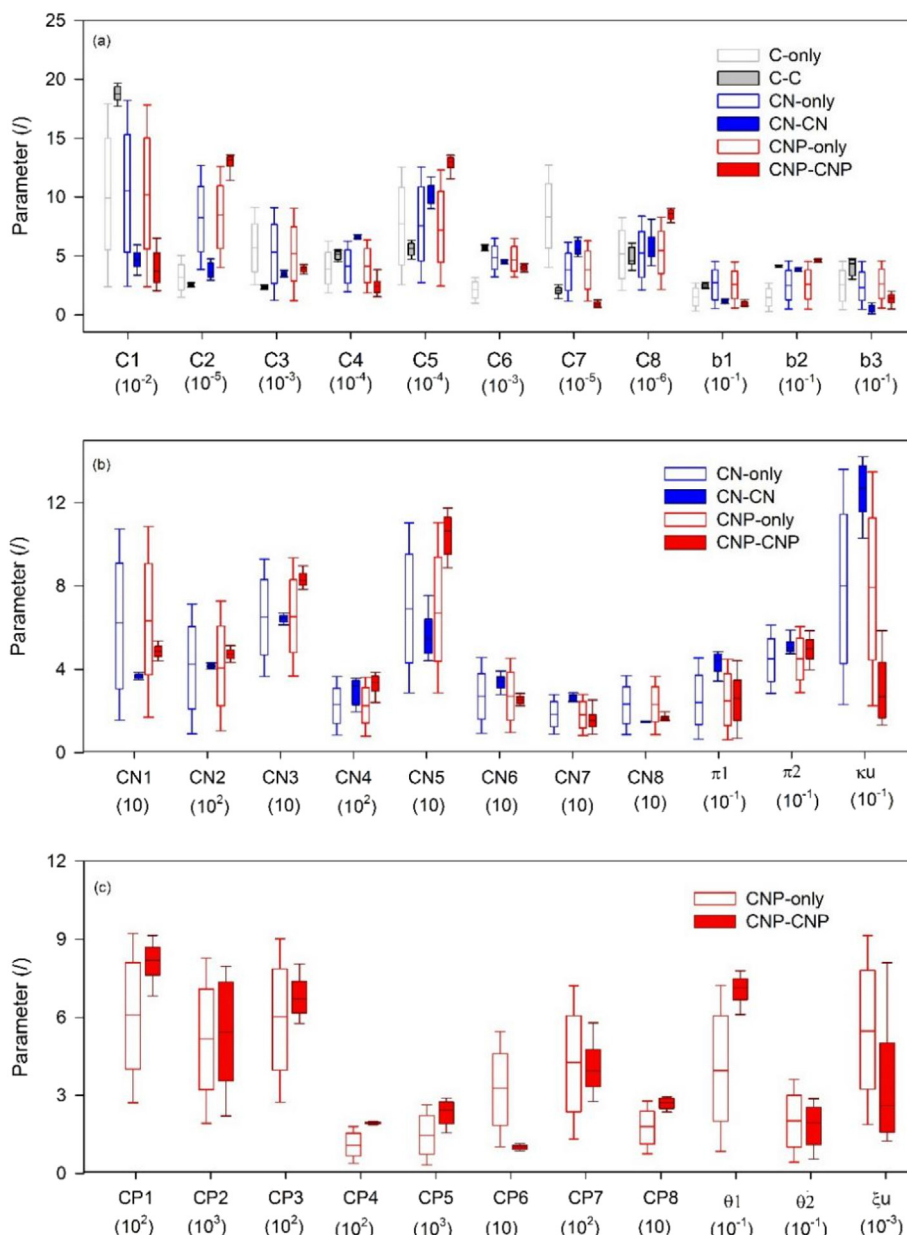


Fig. 3. Median (central line), 25 to 75% range (wide boxes), 5 to 95% range (whiskers) for 11 parameters relating to carbon (C) cycle across all six experiments (panel a), for 11 parameters relating to nitrogen (N) cycle in four experiments (i.e., CN-only, CN-CN, CNP-only and CNP-CNP, respectively, panel b), and for 11 parameters relating to phosphorus (P) cycle in both CNP-only and CNP-CNP (panel c) in the QYZ site. See Table S1 for parameter abbreviations and units.

total C storage (−47.9%), and added N processes affected the fast (−169%), slow (−95%) and passive (−118%) SOM pools and total C storage (−44.2%) (Fig. 6b). Additional P processes induced less effects on most C pools except total C storage (+21.9% vs −2.6%) compared with the added P data in QYZ site (Fig. 6d). For both sites, the offset between nutrient data and processes decreased the combined effects of nutrient modules on most C pools as well as the total C storage. Nevertheless, added N module induced the negative effects on woody biomass, which was the largest contribution on total C storage for both Tiantong (−40.9%) and QYZ (−56.4%) sites. The P module induced negative effect on metabolic litter (−49.9%) in Tiantong site and positive effect on slow SOM (+51.1%) in QYZ site, which were also the largest contribution on total C storage.

The information contributions (i.e., relative information gain [RIG]) of additional nutrient modules from data sets and processes were quantified by Shannon information index (SII, Eq. (5), Fig. 7). In both Tiantong and QYZ sites, added N data, N processes, and both N data

and process induced the biggest RIGs for passive SOM (0.15 bit for Tiantong and 0.96 bit for QYZ), slow SOM (0.03 and 0.1 bit), and passive SOM (0.12 and 0.52bit) pools, respectively. The biggest RIGs were from slow SOM (0.68 bit), structural litter (0.09 bit) and slow SOM (0.59 bit) pools as a result of added P data, P processes and both in Tiantong site, respectively, while the passive SOM (0.83 bit), structural litter (0.13 bit) and passive SOM (0.4 bit) were the biggest RIGs induced by P data, processes and both, respectively.

4. Discussion

4.1. Effects of N vs. P limitation on ecosystem C storage in two subtropical forests

This study evaluated the determinants of nutrient status in subtropical forests by gradually integrating nutrient processes and measurements in a model-data fusion framework. The results demonstrated

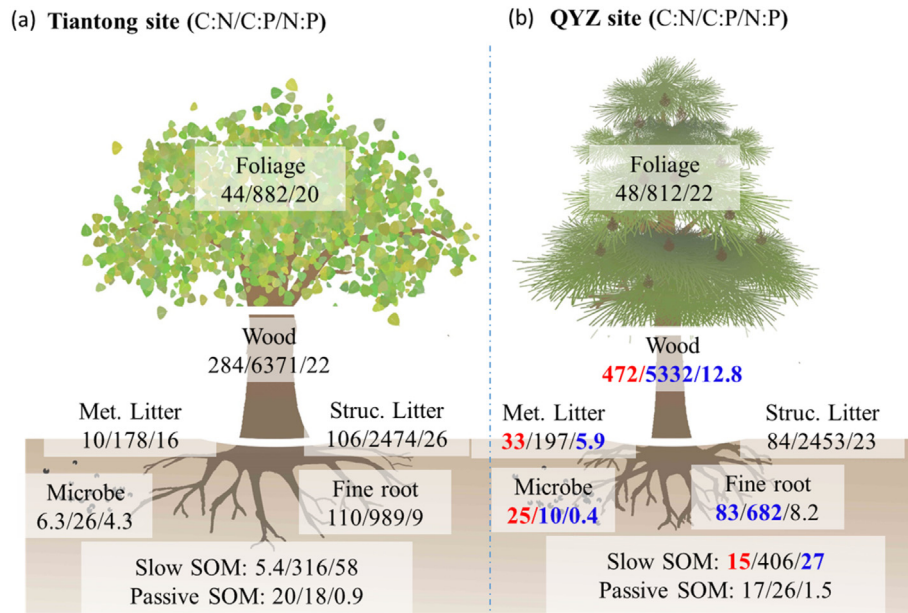


Fig. 4. The stoichiometry (C:N ratio, C:P ratio and N:P ratio) of C pools for (panel a) phosphorus (P) limited site (Tiantong) and (panel b) nitrogen (N) limited site (QYZ). The values in bold red in panel b indicate they are significantly higher in QYZ site than those in Tiantong site, while the bold-blue values indicate they are significantly lower in QYZ site than those in Tiantong site.

that Tiantong site was dominantly P-limited while effects of N limitation decreased ecosystem C storage projections in QYZ site. Therefore, the indicators of N- and P-dominated limitations under natural ecosystems could be distinguished and the underlying mechanisms behind the different nutrient stress could be recognized.

Our approach effectively distinguished effects of N and P limitations according to two lines of evidence. First, N limitation dominantly

decreased the C storage projections in QYZ site, but P limitation did in Tiantong site (Fig. 5). Added P module induced the largest decrease on C sequestration projections in Tiantong site, while added N module induced the greatest constrains in QYZ site. Specifically, the nutrient effects on slow-turnover pools drove long-term C storage trajectories for the both sites but probably with different mechanisms. In Tiantong site, the combination of fast turnover rate of metabolic litter (C_4) and high C allocation rate (b_2) regulated the sizes of metabolic litter and woody biomass in CNP-CNP (Figs. 2a and S3). However, in QYZ site, the C storage projections were regulated by added N module, which constrained the turnover rate of slow SOM (C_7) and allocation of woody biomass (b_2) (Fig. 3). This may be related to slow-turnover pools in woody species acting as nutrient reservoirs, which are more responsive indicators for soil nutrient availability than fast-turnover pools (Garrish et al., 2010; Schreeg et al., 2014). This might be due to that nutrient demands varied for different tree species and/or tree ages between the Tiantong and QYZ sites (Lu et al., 2010; H. Liu et al., 2019; R. Liu et al., 2019). These findings were consistent with the results from the field nutrient addition experiments, demonstrating that responses of C storage to N and P constraints mainly resulted from the difference in soil physical or chemical properties (Vitousek et al., 2010), plant species composition (Huang et al., 2012), and forest succession (Davidson et al., 2007; Yan et al., 2018; Ma et al., 2020) between two subtropical forests.

Second, different effects of N and P limitation were proved by flexible N:P ratios for specific C pools. Specifically, the N:P ratios were higher in Tiantong than in QYZ sites for woody biomass, metabolic and structural litter, microbe and slow SOM, but were not the case for the foliage and fine roots (Fig. 4). The variations of N:P ratios for both plant and SOM pools occurring between the two sites displayed the adaptability of natural ecosystems under different nutrient stress (Sterner and Elser, 2002; Elser et al., 2000; Cleveland and Liptzin, 2007). Different N:P ratios for those slow turnover pools (i.e., wood, structural litter and slow SOM) reflect the imbalanced accumulation of nutrient storage in the two subtropical forest ecosystems. Higher N:P ratios for slow turnover pools indicated relatively less stored P in Tiantong site in comparison with those in QYZ site (Fig. 4). However, low N:P ratios in foliage and fine roots may have illustrated that plants increased the

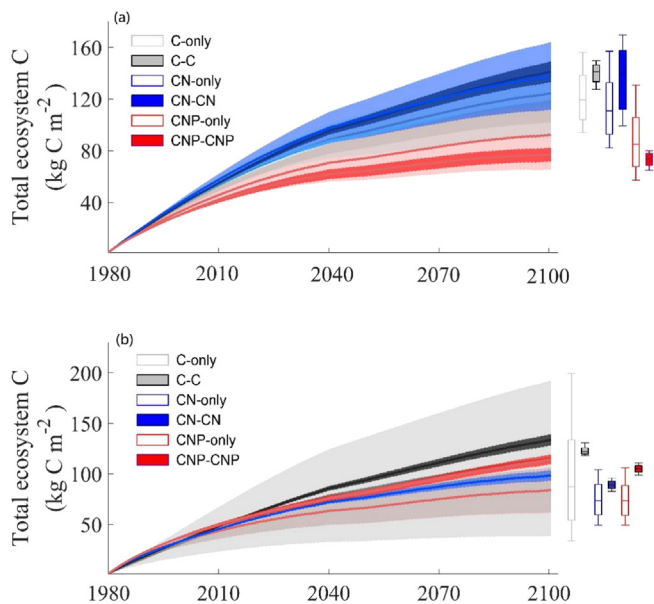


Fig. 5. Total ecosystem carbon (C) dynamics projections in the two subtropical forests, (a) Tiantong site and (b) QYZ site, using 5000 random parameters sampled from posteriori parameter space (C-only, CN-only, CNP-only, C-C, CN-CN and CNP-CNP) used in TECO-C, TECO-CN and TECO-CNP, respectively. The line is mean value and the respective shaded band shows uncertainties (95% confidence intervals) for the spread over 5000 simulations for each experiment. Median (central line), 25 to 75% range (wide boxes), 5 to 95% range (whiskers) for the projections at the end of the projections are shown in the right for each experiment, respectively.

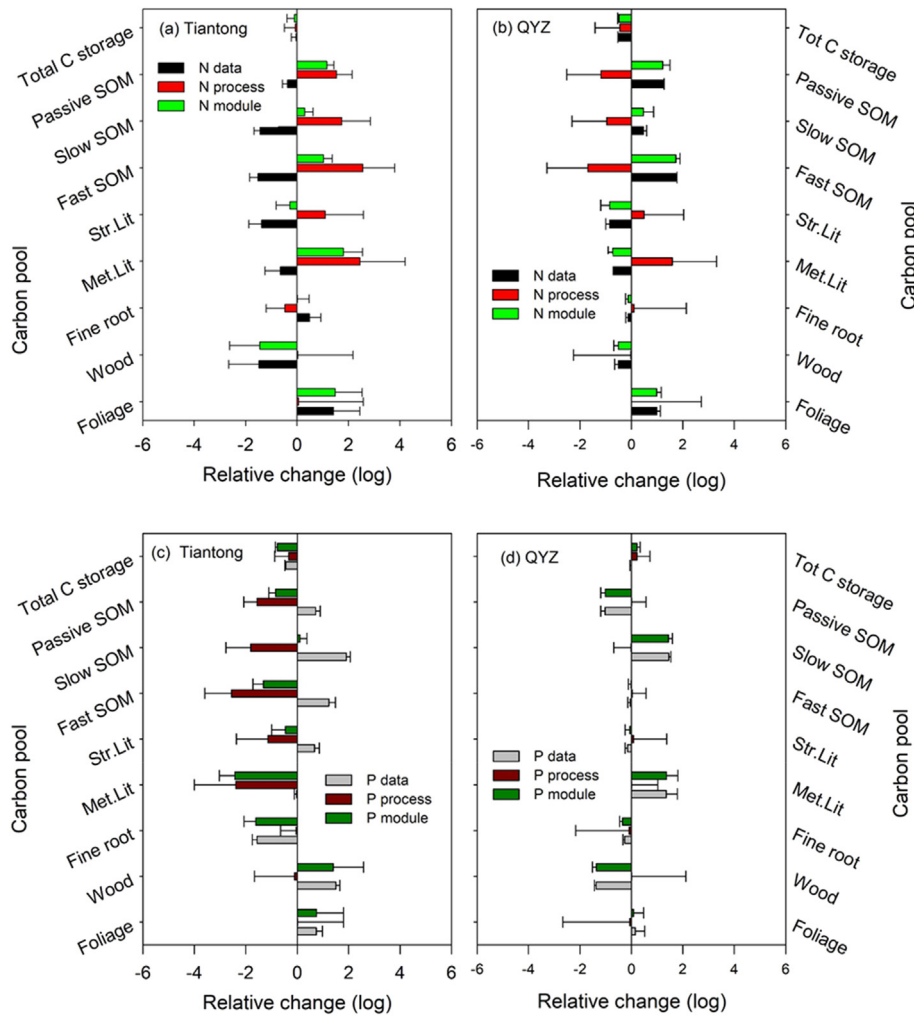


Fig. 6. Effects on carbon (C) pools from nitrogen (N) (a, b) and phosphorus (P) modules (processes, data and both combined) (c, d) at end of prediction (2100) in Tiantong site and QYZ site, respectively. Met. Lit, metabolic litter; Str. Lit, structural litter; SOM, soil organic matter.

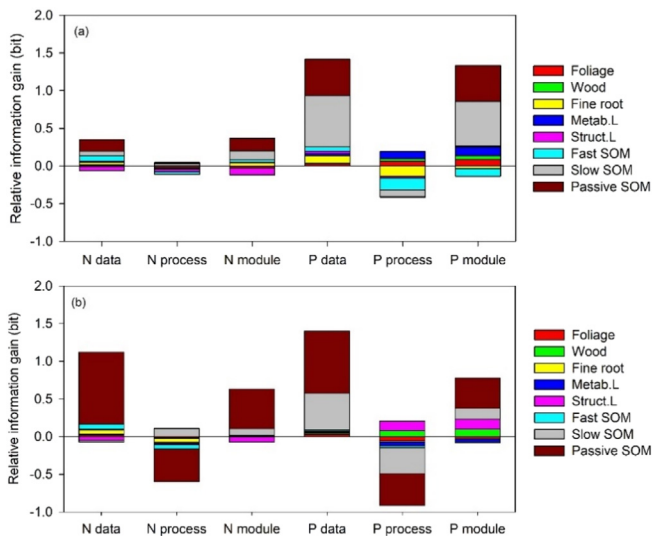


Fig. 7. Relative information gains (D_{KL}) from nitrogen (N) and phosphorus (P) modules (processes, data and both combined) at end of prediction (2100) in the two subtropical forest sites. (a) Tiantong site; (b) QYZ site; Metabolic litter (Metab. L); structural litter (Struct. L); soil organic matter (SOM).

degree of P availability following those fast-turnover tissues in P-limited site. We also found a higher N:P ratio in litter and further led to higher N:P ratios in SOM in Tiantong than QYZ sites (Fig. 4), implying that P-limited trees tended to serve more P from both fine roots and leaves prior to abscission. This is probably due to the fact that nutrient relocation is an important mechanism in the subtropical forest ecosystems to retain N or P in plant developing tissues (Escudero et al., 1992; Aerts, 1996; Crous et al., 2019; Xu et al., 2020). Those findings were consistent with previous studies that the amount of both N and P resorption tend to increase under nutrient stress (Reed et al., 2012; Vergutz et al., 2012; Du et al., 2020). In contrast, our results revealed that N:P ratios of fast turnover pools in plant parts (e.g., leaf and fine root) should not be treated as indicators for nutrient limitation in a given ecosystem (de Campos et al., 2013; Crous et al., 2019).

As nutrient cycling in natural ecosystems is largely driven by the microorganisms (Waldrop and Firestone, 2004; Spohn et al., 2016), both the stoichiometry and activity of microbes are related to resource acquisition and are usually used as predictors of nutrient limitation (Cleveland and Liptzin, 2007; Sinsabaugh et al., 2009; Waring et al., 2013). There was a considerable difference in the N:P ratio of microbial biomass between the two sites (Fig. 4). The added P-related measurements in Tiantong site showed a high sensitivity of the total C to the microbial C:P ratio ($R^2 = 0.72$, Fig. S3). In contrast, added N-related data led to a high sensitivity of the total C to the microbial turnover rate (C_6 , $R^2 = 0.57$, Fig. S4) in the QYZ site. Those results suggested that

the P- and N-related measurements contained different information in constraining the stoichiometry of soil microorganisms, which could be treated as an indicator of nutrient limiting. Those findings were supported by a long-term fertilization experiment in forest ecosystems, in which plant production and litter decomposition were limited by N and/or P availability largely due to soil ages, driving both the stoichiometry and activities of soil microorganisms (Vitousek and Farrington, 1997; Hobbie et al., 2007; He et al., 2020).

4.2. N and P effects on C storage projections

The different effects of N and P limitations on C storage projections between the two subtropical forest ecosystems reflected that the biogeochemical processes were associated with vegetation type, soil type, nutrient acquisition strategy of plants and microbes, and soil nutrient availability. Distinguishing the N and P effects via model intercomparison in the TECO framework can provide a unique opportunity to quantify the effects of nutrient availability and limitation on ecosystem C processes.

The plant photosynthetic capacity is also associated with the leaf N and P concentrations, reflecting plant investment in photosynthetic machinery for light harvesting and carboxylation rates (Walker et al., 2014; Bahar et al., 2017; Yan et al., 2018). In this study, we assumed the same nutrient effects on GPP at the two sites, since we used the identical GPP as model forcing for all the TECO versions (Fig. 1). However, both added N and P modules increased the size of foliage C pools in the two sites (Fig. 6), mostly due to a decrease in foliar turnover rate (C_1 , Figs. 2, 3, S3 and S4). Integrating N- and P-modules prolong the leaf life span, leading to increased plant nutrient use efficiency (Liu et al., 2013; Norby et al., 2017). Tiantong site had the higher variation in foliar turnover rate than QYZ site (Figs. 2 and 3), which supported the idea that the weaker homeostatic control existed in leaf turnover due to different tree species and the stand age (Kattge et al., 2009; Garrish et al., 2010; Liu et al., 2013).

Both N- and P-modules induced large effects on woody biomass for the two sites (Fig. 6), but with different mechanisms. In the Tiantong site, added N module decreased the woody pool size, which was mainly driven by decreased woody C allocation (b_2) (Figs. 2 and S3). On the contrary, added P module induced positive effect mainly due to increased C allocation to woody tissue. However, in QYZ site, both added N- and P-modules increased the turnover rate of woody (C_2), resulting in the negative effects of the woody pool (Figs. 3 and S4). Those different effects on woody tissue further affected C transfer to the metabolic litter and slow SOM in Tiantong and QYZ sites (Fig. 6), respectively. One possible reason is the difference of nutrient use strategies between the two sites with the different stand ages. That is, under nutrient stress, older stands in Tiantong site tend to adjust element allocation to maintain the stoichiometric balance, while younger stands in QYZ site accelerated the turnover of nonphotosynthetic tissues (e.g., woody and root). Another reason may be the species-specific nutrient economy under different environmental conditions (Wright and Westoby, 2003; Reed et al., 2012; Yan et al., 2018). The tradeoff of turnover (including allocation and decomposition) between woody and metabolic litter would be a strategy for the evergreen broadleaf forest in Tiantong site under unbalanced N and P conditions (Li et al., 2016; Camenzind et al., 2018). However, for the evergreen coniferous forest in QYZ site, faster turnover rate of wood decomposition and higher soil C accumulation seemed to be main mechanism to relieve the effects of nutrient limitation compared with those in Tiantong site (Deng et al., 2017; Kou et al., 2018).

4.3. Model uncertainties from nutrient modules

Models have the potential to explore effects of multiple ecological processes and evaluate the likelihood of future projections (Luo et al., 2011). However, model performance can be influenced by both

additional process and data (Wieder et al., 2014; Hararuk et al., 2015; Du et al., 2017). In this study, we explored the sources of uncertainty in the N and P modules with respect to the data and processes in the two subtropical forest sites by quantifying the differences in relative information among six experiments of TECO model. Overall, the nutrient data offered the beneficial information (i.e., positive information gain) while the added nutrient processes increased noise (i.e., negative information gain) for most C pools in long-term projections in both sites (Fig. 7). Additional observational data provided complementary information for parameter constraint while added processes induced less identifiable information (e.g., fewer constrained parameters), which were consistent with those from previous studies (Thomas et al., 2015; Du et al., 2015, 2017). For instance, additional processes of N and P resulted in negative information gain, while added N and P data induced positive information gain for projections of SOM pools in the two sites. Similarly, the total SOM amount was partitioned into three pools (i.e., fast, slow and passive SOM), inducing high model uncertainty with more parameters, whereas both the N- and P-related data for SOM provided complementary information to constrain those parameters (Figs. 2 and 3). However, the negative information gain from additional nutrient data also existed in a few pools in both sites, such as the metabolic and structural litter (Fig. 7), suggesting that the information contained in the nutrient data was insufficient to separate these two litter pools.

Currently, most biogeochemical models follow a similar structure for the C-N coupling to the TECO model, such as DAYCENT, G-DAY, O-CN, LPJ-GUESS and TECO, but only a few models were incorporated into P processes (e.g., CABLE, DNDC, Wang et al., 2010; Gilhespy et al., 2014). Previous studies have demonstrated that those models can be used to interpret terrestrial ecosystem dynamics in response to observed or manipulated environmental change. The existed models with P process are difficult to incorporate observation into models to estimate parameters and assess the model structure. We thus implanted the P module in our TECO model to examine effects of nutrient limitation on C storage capacity. Despite specific representations of some processes in the TECO model framework (e.g., a much larger SOM pool) compared with other models, our analysis still showed an improvement in quantifying the different patterns of nutrient limitation between two subtropical forest ecosystems by adding nutrient modules in terrestrial ecosystem models.

5. Conclusions

Improving representation of nutrient limitation is a high priority for ecosystem and land surface modeling, especially when these models simulate responses of C storage capacity to imbalanced N and P inputs. In this study, we investigated the effects of the N- and P-modules on C storage capacities by gradually integrating nutrient processes and measurements in a model-data fusion framework at two subtropical forests. The results showed that P dominantly constrained C storage capacities in Tiantong whereas the N limitation decreased C storage projections in QYZ site. Stoichiometry of wood biomass and soil microbe were good indicators of N/P availability under natural ecosystems. These findings suggest that the distinct nutrient demands for different trees species and tree ages, and representation of flexible stoichiometries for both slow-turnover pools and soil microbe are essential to improve ecosystem C storage projection in the future.

Code availability

The code for TECO-C, TECO-CN and TECO-CNP is available at https://github.com/zgdu/MCMC_TECO-CNP (last access: 4 November 2020).

Data availability

The data for this paper are available upon request to the corresponding authors.

CRedit authorship contribution statement

ZD and XZ designed the study. XZ, GZ, LZ, HW and GY provided measurement data. ZD and JW wrote the code and performed the experiments. ZD wrote the paper with contributions from all coauthors.

Declaration of competing interest

The authors declare that they have no conflict of interest.

Acknowledgements

This research was financially supported by the National Natural Science Foundation of China (Grant No. 31930072, 32071593, 31722009, 31600352), the Program for Professor of Special Appointment (Eastern Scholar) at Shanghai Institutions of Higher Learning, “Thousand Young Talents” Program in China, and the fellowship of China Postdoctoral Science Foundation (Grant No. 2020M681235).

Appendix A. Data assimilation

We used a Bayesian inversion approach which built upon the Bayesian probabilistic inversion to assimilate the observed datasets into the models. Bayes' theorem states that the posterior probability density function (PDF) $p(c|Z)$ of model parameters c can be obtained from prior knowledge of parameters and information generated by a comparison of simulated and observed variables. The theorem can be expressed as follows:

$$p(c|Z) = \frac{p(Z|c)p(c)}{p(Z)} \tag{A1}$$

where $p(c)$ is the prior probability density distribution PDF, $p(c|Z)$ represents the probability of the observed data, and $p(Z|c)$ is the likelihood function for parameter c that expresses the fit between the modeled and observed data. The prior PDF of the estimated parameters $p(c)$ was specified as the uniform distribution over a set of specific intervals (see Table 1). Lower and upper limits of the intervals were set by synthesizing values from the literature, knowledge of the system, the raw model output, and prior information from Luo et al. [2003], Wu et al. [2009] and Shi et al. [2016]. The likelihood function $p(Z|c)$ was calculated with the assumption that observation errors followed a Gaussian distribution with a zero mean (Eq. (3)). The error for each modeled value $X_i(t)$ compared with the observed value $Z_i(t)$ at time t , expressed by

$$e_i = Z_i(t) - Y_i(t) \tag{A2}$$

To calculate $Y_i(t)$ from the modeled data $X_i(t)$, we used the mapping operator $\Phi = (\varphi_1^T, \varphi_2^T, \dots, \varphi_9^T)^T$ to match the simulated state variables (C and N contents of the eight pools) and fluxes to the observational variables at time t (Luo et al., 2003; Du et al., 2015; Shi et al., 2016), and Φ is a 9×8 matrix given as

$$\Phi = \begin{pmatrix} 0.75 & 0 & 0 & 0 & 0 & 0 & 0 & 0 \\ 0 & 1 & 0 & 0 & 0 & 0 & 0 & 0 \\ 0 & 0 & 0.75 & 0 & 0 & 0 & 0 & 0 \\ c_1 & 0 & 0 & 0 & 0 & 0 & 0 & 0 \\ 0 & 0 & 0 & 0.75 & 0.75 & 0 & 0 & 0 \\ 0 & 0 & 0 & 0 & 0 & 1 & 0 & 0 \\ 0 & 0 & 0 & 0 & 0 & 1 & 1 & 1 \\ 0.25c_1 & 0.25c_2 & 0.25c_3 & 0.55c_4 & 0.45c_5 & 0.7c_6 & 0.55c_7 & 0.55c_8 \\ 0 & 0 & 0 & 0.55c_4 & 0.45c_5 & 0.7c_6 & 0.55c_7 & 0.55c_8 \end{pmatrix} \tag{A4}$$

For the each pool or flux, the modeled value was expressed as

$$Y_i = \varphi_i X(i), i = 1, 2, \dots, 9 \tag{A5}$$

The posterior PDFs $p(c|Z)$ for the model parameters were generated from prior PDFs $p(c)$ with observations Z using a Markov chain Monte Carlo (MCMC) sampling technique. The Metropolis-Hastings (M-H) algorithm [Metropolis et al., 1953; Hastings, 1970] was used as the MCMC sampler. New proposal parameter points were generated by:

$$c^{new} = c^{k-1} + r(\theta_{max} - \theta_{min}) \tag{A7}$$

where θ_{max} and θ_{min} are the maximum and minimum values of the given parameter space, respectively, and r is a random variable between -0.5 and 0.5 with a uniform distribution. Whether the new point c^{new} was accepted or not dependent on the value of the ratio $R = \frac{p(c^{new}|Z)}{p(c^{k-1}|Z)}$ compared with a uniform random number N from 0 to 1. Only if $R \geq N$, the new point was accepted (i.e., $c^k = c^{new}$); otherwise $c^k = c^{k-1}$ (Xu et al., 2006). We formally made five parallel runs using the M-H algorithm with 600,000 simulations for each run. Each run started from a random initial point in parameter spaces to eliminate the effect of the initial condition on stochastic sampling. The acceptance rates for the five runs tested by the Gelman-Rubin (G-R) diagnostic method in the three experiments ranged from 5% to 10% (Xu et al., 2006). The initial samples (approximately 6000 for each run) were discarded after the running means and standard deviations (SDs) were stabilized (regarded as the burn-in period).

All the accepted samples from five runs after the burn-in periods (approximately 100,000 samples in total) in each experiment were used to construct posterior PDFs. The same sets of simulated C contents of the eight pools were generated by 98-year forward model runs with these accepted parameters.

Appendix B. Supplementary data

Supplementary data to this article can be found online at <https://doi.org/10.1016/j.scitotenv.2021.148485>.

References

Aerts, R., 1996. Nutrient resorption from senescing leaves of perennials: are there general patterns? *J. Ecol.* 84, 597–608.
 Ahlström, A., Schurgers, G., Arneith, A., Smith, B., 2012. Robustness and uncertainty in terrestrial ecosystem carbon response to CMIP5 climate change projections. *Environ. Res. Lett.* 7 (4), 044008.
 Arneith, A., Harrison, S.P., Zaehle, S., Tsigaridis, K., Menon, S., Bartlein, P.J., Schurgers, G., 2010. Terrestrial biogeochemical feedbacks in the climate system. *Nat. Geosci.* 3 (8), 525–532.

Table 1
The biometric data sets that were assimilated in this study.

Variable	Tiantong		QYZ		Unit
	Size of data	Mean ± std	Size of data	Mean ± std	
Soil respiration	41	2.3 ± 1.6	157	2.2 ± 1.1	$g\ C\ m^{-2}d^{-1}$
Litterfall C	4	435 ± 42.7	7	923 ± 122	$g\ C\ m^{-2}y^{-1}$
Wood C	4	8671 ± 564	7	6606 ± 1051	$g\ C\ m^{-2}$
foliage C	4	217 ± 18.6	7	419 ± 66	$g\ C\ m^{-2}$
Mircobe C	5	164 ± 18.0	4	97.5 ± 9.1	$g\ C\ m^{-2}$
SOC	4	3561 ± 667	2	3944 ± 118	$g\ C\ m^{-2}$
Litterfall N	5	6.7 ± 0.7	7	9.6 ± 1.0	$g\ N\ m^{-2}y^{-1}$
Wood N	4	31.4 ± 2.0	7	15.4 ± 2.4	$g\ N\ m^{-2}$
Leaf N	4	6.1 ± 0.5	6	11.7 ± 1.9	$g\ N\ m^{-2}$
Soil TN	11	581 ± 69	4	107 ± 24	$g\ N\ m^{-2}$
Inorganic N	8	3.4 ± 0.6	5	2.2 ± 0.5	$g\ N\ m^{-2}$
Litterfall P	5	0.8 ± 0.2	5	1.08 ± 0.1	$g\ P\ m^{-2}y^{-1}$
Wood P	4	1.7 ± 0.1	4	1.8 ± 0.3	$g\ P\ m^{-2}$
Leaf P	4	0.7 ± 0.1	4	0.5 ± 0.1	$g\ P\ m^{-2}$
Soil TP	11	34.7 ± 4.1	3	46.7 ± 6.3	$g\ P\ m^{-2}$

- Arora, V.K., Boer, G.J., Friedlingstein, P., et al., 2013. Carbon-concentration and carbon-climate feedbacks in CMIP5 earth system models. *J. Clim.* 26 (15), 5289–5314.
- Averill, C., Waring, B., 2018. Nitrogen limitation of decomposition and decay: how can it occur? *Glob. Chang. Biol.* 24 (4), 1417–1427.
- Bahar, N.H., Ishida, F.Y., Weerasinghe, L.K., et al., 2017. Leaf-level photosynthetic capacity in lowland Amazonian and high-elevation Andean tropical moist forests of Peru. *New Phytol.* 214, 1002–1018.
- Bai, S.H., Xu, Z., Blumfield, T.J., Reverchon, F., 2015. Human footprints in urban forests: implication of nitrogen deposition for nitrogen and carbon storage. *J. Soils Sediments* 15 (9), 1927–1936.
- Camenizind, T., Hättenschwiler, S., Treseder, K.K., Lehmann, A., Rillig, M.C., 2018. Nutrient limitation of soil microbial processes in tropical forests. *Ecol. Monogr.* 88 (1), 4–21.
- Cleveland, C.C., Liptzin, D., 2007. C:N:P stoichiometry in soil: is there a "Redfield ratio" for the microbial biomass? *Biogeochemistry* 85, 235–252.
- Cleveland, C.C., Townsend, A.R., Schmidt, S.K., 2002. Phosphorus limitation of microbial processes in moist tropical forests: evidence from short-term laboratory incubations and field studies. *Ecosystems* 5, 0680–0691.
- Craine, J.M., et al., 2009. Global patterns of foliar nitrogen isotopes and their relationships with climate, mycorrhizal fungi, foliar nutrient concentrations, and nitrogen availability. *New Phytol.* 183, 980–992.
- Crous, K.Y., Wujeska-Klause, A., Jiang, M., et al., 2019. Nitrogen and phosphorus retranslocation of leaves and stemwood in a mature Eucalyptus forest exposed to 5 years of elevated CO₂. *Front. Plant Sci.* 10.
- Dai, X., Fu, X., Kou, L., Wang, H., Shock, C.C., 2018. C:N:P stoichiometry of rhizosphere soils differed significantly among overstory trees and understory shrubs in plantations in subtropical China. *Can. J. For. Res.* 48 (11), 1398–1405.
- Davidson, E.A., de Carvalho, C.J., Figueira, A.M., et al., 2007. Recuperation of nitrogen cycling in Amazonian forests following agricultural abandonment. *Nature* 447, 995–998.
- de Campos, M.C.R., Pearse, S.J., Oliveira, R.S., Lambers, H., 2013. Downregulation of net phosphorus-uptake capacity is inversely related to leaf phosphorus-resorption proficiency in four species from a phosphorus-impooverished environment. *Ann. Bot.* 111, 445–454.
- Deng, Q., Hui, D., Dennis, S., Reddy, K.C., 2017. Responses of terrestrial ecosystem phosphorus cycling to nitrogen addition: a meta-analysis. *Glob. Ecol. Biogeogr.* 26 (6), 713–728.
- Du, Z., Nie, Y., He, Y., Yu, G., Wang, H., Zhou, X., 2015. Complementarity of flux- and biometric-based data to constrain parameters in a terrestrial carbon model. *Tellus Ser. B* 67, 24102.
- Du, Z., Zhou, X., Shao, J., Yu, G., Wang, H., Zhai, D., Xia, J., Luo, Y., 2017. Quantifying uncertainties from additional nitrogen data and processes in a terrestrial ecosystem model with Bayesian probabilistic inversion. *J. Adv. Model. Earth Syst.* 09. <https://doi.org/10.1002/2016MS000687>.
- Du, Z., Weng, E., Jiang, L., Luo, Y., Xia, J., Zhou, X., 2018. Carbon-nitrogen coupling under three schemes of model representation: a traceability analysis. *Geosci. Model Dev.* 11 (11), 4399–4416.
- Du, E., Terrer, C., Pellegrini, A.F.A., Ahlström, A., van Lissa, C.J., Zhao, X., ... Jackson, R.B., 2020. Global patterns of terrestrial nitrogen and phosphorus limitation. *Nat. Geosci.* 13 (3), 221–226.
- Elser, J.J., O'Brien, W.J., Dobberfuhl, D.R., Dowling, T.E., 2000. The evolution of ecosystem processes: growth rate and elemental stoichiometry of a key herbivore in temperate and arctic habitats. *J. Evol. Biol.* 13, 845–853.
- Escudero, A., Delarco, J.M., Sanz, I.C., Ayala, J., 1992. Effects of leaf longevity and retranslocation efficiency on the retention time of nutrients in the leaf biomass of different woody species. *Oecologia* 90, 80–87.
- Fan, H.B., Wu, J.P., Liu, W.F., Yuan, Y.H., Hu, L., Cai, Q.K., 2015. Linkages of plant and soil C:N:P stoichiometry and their relationships to forest growth in subtropical plantations. *Plant Soil* 392, 127–138.
- Finzi, A.C., Moore, D.J.P., DeLucia, E.H., et al., 2006. Progressive nitrogen limitation of ecosystem processes under elevated CO₂ in a warm-temperate forest. *Ecology* 87 (1), 15–25.
- Friedlingstein, P., Cox, P., Betts, R., Bopp, L., von Bloh, W., Brovkin, V., Bala, G., 2006. Climate-carbon cycle feedback analysis: results from the C4MIP model intercomparison. *J. Clim.* 19 (14), 3337–3353.
- Galloway, J.N., Dentener, F.J., Capone, D.G., Boyer, E.W., Howarth, R.W., Seitzinger, S.P., ... Karl, D.M., 2004. Nitrogen cycles: past, present, and future. *Biogeochemistry* 70 (2), 153–226.
- Gao, Q., Hasselquist, N.J., Palmroth, S., Zheng, Z., You, W., 2014. Short-term response of soil respiration to nitrogen fertilization in a subtropical evergreen forest. *Soil Biol. Biochem.* 76, 297–300.
- Gao, Y., Hao, Z., Yang, T., He, N., Wen, X., Yu, G., 2017. Effects of atmospheric reactive phosphorus deposition on phosphorus transport in a subtropical watershed: a Chinese case study. *Environ. Pollut.* 226, 69–78.
- Garrish, V., Cernusak, L.A., Winter, K., Turner, B.L., 2010. Nitrogen to phosphorus ratio of plant biomass versus soil solution in a tropical pioneer tree, *Ficus insipida*. *J. Exp. Bot.* 61, 3735–3748.
- Gilhespy, S.L., Anthony, S., Cardenas, L., Chadwick, D., del Prado, A., Li, C., ... Sanz-Cobena, A., 2014. First 20 years of DNDC (DeNitrification DeComposition): model evolution. *Ecol. Model.* 292, 51–62.
- Hastings, W.K., 1970. Monte Carlo Sampling methods using Markov chains and their Applications. *Biometrika* 57 (1), 97–109.
- Hararuk, O., Smith, M.J., Luo, Y., 2015. Microbial models with data-driven parameters predict stronger soil carbon responses to climate change. *Glob. Chang. Biol.* 21, 2439–2453.
- He, X., Hou, E., Veen, G.F., Ellwood, M.D.F., Dijkstra, P., Sui, X., ... Chu, C., 2020. Soil microbial biomass increases along elevational gradients in the tropics and subtropics but not elsewhere. *Glob. Ecol. Biogeogr.* 29 (2), 345–354.
- Hobbie, S.E., Ogdahl, M., Chorover, J., Chadwick, O.A., Oleksyn, J., Zytzkowski, R., Reich, P.B., 2007. Tree species effects on soil organic matter dynamics: the role of soil cation composition. *Ecosystems* 10, 999–1018.
- Huang, M., Ji, J., Li, K., Liu, Y., Yang, F., et al., 2007. The ecosystem carbon accumulation after conversion of grasslands to pine plantations in subtropical red soil of South China. *Tellus B* 59, 439–448.
- Huang, W.J., Zhou, G.Y., Liu, J.X., 2012. Nitrogen and phosphorus status and their influence on aboveground production under increasing nitrogen deposition in three successional forests. *Acta Oecol.* 44, 20–27.
- Hungate, B.A., Dukes, J.S., Shaw, R., Luo, Y., Field, C.B., 2003. Nitrogen and climate change. *Science* 302, 1512–1513.
- Jia, Y., Yu, G., He, N., Zhan, X., Fang, H., Sheng, W., Zuo, Y., Zhang, D., Wang, Q., 2014. Spatial and decadal variations in inorganic nitrogen wet deposition in China induced by human activity. *Sci. Rep.* 4, e3763.
- Jiang, X., Liu, N., Lu, X., Huang, J.-G., Cheng, J., Guo, X., Wu, S., 2018. Canopy and understory nitrogen addition increase the xylem tracheid size of dominant broadleaf species in a subtropical forest of China. *Sci. Total Environ.* 642, 733–741.
- Kattge, J., Knorr, W., Raddatz, T., Wirth, C., 2009. Quantifying photosynthetic capacity and its relationship to leaf nitrogen content for global-scale terrestrial biosphere models. *Glob. Chang. Biol.* 15 (4), 976–991.
- Kou, L., Jiang, L., Fu, X., Dai, X., Wang, H., Li, S., 2018. Nitrogen deposition increases root production and turnover but slows root decomposition in *Pinus elliotii* plantations. *New Phytol.* 218 (4), 1450–1461.
- Kou-Giesbrecht, S., Menge, D., 2019. Nitrogen-fixing trees could exacerbate climate change under elevated nitrogen deposition. *Nat. Commun.* 10, 1493. <https://doi.org/10.1038/s41467-019-09424-2>.
- Kullback, S., Leibler, R.A., 1951. On information and sufficiency. *Ann. Math. Stat.* 22 (1), 79–86.
- Lebauer, D.S., Treseder, K.K., 2008. Nitrogen limitation of net primary productivity in terrestrial ecosystems is globally distributed. *Ecology* 89, 371–379.
- Li, X.R., Liu, Q.J., Chen, Y., Hu, L., Yang, F., 2006. Aboveground biomass of three conifers in Qianyanzhou plantation. *Chin. J. Appl. Ecol.* 17 (8), 1382–1388.
- Li, Y., Niu, S., Yu, G., 2016. Aggravated phosphorus limitation on biomass production under increasing nitrogen loading: a meta-analysis. *Glob. Chang. Biol.* 22 (2), 934–943.
- Liu, J.X., Huang, W.J., Zhou, G.Y., Zhang, D.Q., 2013. Nitrogen to phosphorus ratios of tree species in response to elevated carbon dioxide and nitrogen addition in subtropical forests. *Glob. Chang. Biol.* 19, 208–216.
- Liu, H., Zhou, G., Bai, S.H., Song, J., Shang, Y., He, M., ... Zheng, Z., 2019a. Differential response of soil respiration to nitrogen and phosphorus addition in a highly phosphorus-limited subtropical forest, China. *For. Ecol. Manag.* 448, 499–508. <https://doi.org/10.1016/j.foreco.2019.06.020>.
- Liu, R., Zhou, X., Wang, J., Shao, J., Fu, Y., Liang, C., et al., 2019b. Differential magnitude of rhizosphere effects on soil aggregation at three stages of subtropical secondary forest successions. *Plant Soil* 436 (1), 365–380.
- Lu, X., Mo, J., Gilliam, F.S., Zhou, G., Fang, Y., 2010. Effects of experimental nitrogen additions on plant diversity in an old-growth tropical forest. *Glob. Chang. Biol.* 16, 2688–2700.
- Luo, Y., Reynolds, J.F., 1999. Validity of extrapolating field CO₂ experiments to predict carbon sequestration in natural ecosystems. *Ecology* 80, 1568–1583.
- Luo, Y., White, L.W., Canadell, J.G., Delucia, E.H., Ellsworth, D.S., Finzi, A.C., et al., 2003. Sustainability of terrestrial carbon sequestration: a case study in Duke Forest with inversion approach. *Glob. Biogeochem. Cycles* 17 (1), 1021.
- Luo, Y., Su, B., Currie, W.S., Dukes, J.S., Finzi, A.C., Hartwig, U., Hungate, B.A., McMurtrie, R.E., Oren, R., Parton, W.J., Pataki, D.E., Shaw, M.R., Zak, D.R., Field, C.B., 2004. Progressive nitrogen limitation of ecosystem responses to rising atmospheric carbon dioxide. *Bioscience* 54, 731–739.
- Luo, Y., Hui, D., Zhang, D., 2006. Elevated CO₂ stimulates net accumulations of carbon and nitrogen in land ecosystems: a meta-analysis. *Ecology* 87, 53–63.
- Luo, Y., Ogle, K., Tucker, C., Fei, S., Gao, C., La Deau, S., Clark, J., Schimel, D.S., 2011. Ecological forecasting and data assimilation in a data-rich era. *Ecol. Appl.* 21, 1429–1442.
- Ma, S., Eziz, A., Tian, D., Yan, Z., Cai, Q., Jiang, M., Ji, C., Fang, J., 2020. Size- and age-dependent increases in tree stem carbon concentration: implications for forest carbon stock estimations. *J. Plant Ecol.* 13 (2), 233–240. <https://doi.org/10.1093/jpe/rtaa005>.
- Mahowald, N., Jickells, T.D., Baker, A.R., Artaxo, P., Benitez-Nelson, C.R., Bergametti, G., ... Kubilay, N., 2008. Global distribution of atmospheric phosphorus sources, concentrations and deposition rates, and anthropogenic impacts. *Glob. Biogeochem. Cycles* 22 (4).
- Metropolis, N., Rosenbluth, A.W., Rosenbluth, M.N., Teller, A.H., Teller, E., 1953. Equation of state calculations by fast computing machines. *J. Chem. Phys.* 21 (6), 1087–1092.
- Melillo, J.M., Steudler, P.A., Aber, J.D., Newkirk, K., Lux, H., Bowles, F.P., et al., 2002. Soil warming and carbon-cycle feedbacks to the climate system. *Science* 298 (5601), 2173–2176.
- Melillo, J.M., Butler, S., Johnson, J., et al., 2011. Soil warming, carbon-nitrogen interactions, and forest carbon budgets. *Proc. Natl. Acad. Sci.* 108 (23), 9508–9512.
- Mo, X., Dai, X., Wang, H., Fu, X., Kou, L., 2018. Rhizosphere effects of overstory tree and understory shrub species in central subtropical plantations—a case study at Qianyanzhou, Taihe, Jiangxi, China. *Chin. J. Plant Ecol.* 42 (7), 723–733.
- Niu, S., Classen, A.T., Dukes, J.S., et al., 2016. Global patterns and substrate-based mechanisms of the terrestrial nitrogen cycle. *Ecol. Lett.* 19 (6), 697–709.

- Norby, R.J., Warren, J.M., Iversen, C.M., Medlyn, B.E., McMurtrie, R.E., 2010. CO₂ enhancement of forest productivity constrained by limited nitrogen availability. *Proc. Natl. Acad. Sci. USA* 107, 19368–19373.
- Norby, R.J., Gu, L., Haworth, I.C., Jensen, A.M., Turner, B.L., Walker, A.P., ... Winter, K., 2017. Informing models through empirical relationships between foliar phosphorus, nitrogen and photosynthesis across diverse woody species in tropical forests of Panama. *New Phytol.* 215 (4), 1425–1437.
- Omidvar, N., Xu, Z., Nguyen, T.T.N., Salehin, B., Ogbourne, S., Ford, R., Bai, S.H., 2021. A global meta-analysis shows soil nitrogen pool increases after revegetation of riparian zones. *J. Soils Sediments* 21 (2), 665–677.
- Peñuelas, J., Sardans, J., Rivas-ubach, A., Janssens, I.A., 2012. The human-induced imbalance between C, N and P in Earth's life system. *Glob. Chang. Biol.* 18 (1), 3–6.
- Peñuelas, J., Poulter, B., Sardans, J., Ciais, P., van der Velde, M., Bopp, L., Boucher, O., Godderis, Y., Hinsinger, P., Llusia, J., Nardin, E., Vicca, S., Obersteiner, M., Janssens, I.A., 2013. Human-induced nitrogen-phosphorus imbalances alter natural and managed ecosystems across the globe. *Nat. Commun.* 4, 2934.
- Reed, S.C., Townsend, A.R., Davidson, E.A., Cleveland, C.C., 2012. Stoichiometric patterns in foliar nutrient resorption across multiple scales. *New Phytol.* 196, 173–180.
- Reich, P.B., Hobbie, S.E., Lee, T., Ellsworth, D.S., West, J.B., Tilman, D., Knops, J.M.H., Naem, S., Trost, J., 2006. Nitrogen limitation constrains sustainability of ecosystem response to CO₂. *Nature* 440, 922–925.
- Schreeg, L.A., Santiago, L.S., Wright, S.J., Turner, B.L., 2014. Stem, root, and older leaf N:P ratios are more responsive indicators of soil nutrient availability than new foliage. *Ecology* 95 (8), 2062–2068.
- Shi, Z., Yang, Y., Zhou, X., Weng, E., Finzi, A.C., Luo, Y., 2016. Inverse analysis of coupled carbon-nitrogen cycles against multiple datasets at ambient and elevated CO₂. *J. Plant Ecol.* 9, 285–295. <https://doi.org/10.1093/jpe/rtv059>.
- Shi, Z., Crowell, S., Luo, Y., Moore, B., 2018. Model structures amplify uncertainty in predicted soil carbon responses to climate change. *Nat. Commun.* 9, 2171. <https://doi.org/10.1038/s41467-018-04526-9>.
- Sinsabaugh, R.L., Hill, B.H., Follstad Shah, J.J., 2009. Ecoenzymatic stoichiometry of microbial organic nutrient acquisition in soil and sediment. *Nature* 462, 795–798. <https://doi.org/10.1038/nature08632>.
- Spohn, M., Klaus, K., Wanek, W., Richter, A., 2016. Microbial carbon use efficiency and biomass turnover times depending on soil depth – Implications for carbon cycling. *Soil Biol. Biochem.* 96 (96), 74–81.
- Sterner, R.W., Elser, J.J., 2002. *Ecological Stoichiometry: The Biology of Elements From Molecules to the Biosphere*. Princeton University Press, Princeton, NJ.
- Thomas, R.Q., Brookshire, E.J., Gerber, S., 2015. Nitrogen limitation on land: how can it occur in Earth system models? *Glob. Chang. Biol.* 21 (5), 1777–1793.
- Thornton, P.E., Doney, S.C., Lindsay, K., et al., 2009. Carbon-nitrogen interactions regulate climate-carbon cycle feedbacks: results from an atmosphere-ocean general circulation model. *Biogeosciences* 6, 2099–2120.
- Tian, J., Dungait, J.A.J., Lu, X., et al., 2019. Long-term nitrogen addition modifies microbial composition and functions for slow carbon cycling and increased sequestration in tropical forest soil. *Glob. Chang. Biol.* 25 (10), 3267–3281.
- Vergutz, L., Manzoni, S., Porporato, A., Novais, R.F., Jackson, R.B., 2012. Global resorption efficiencies and concentrations of carbon and nutrients in leaves of terrestrial plants. *Ecol. Monogr.* 82, 205–220.
- Vigulu, V., Blumfield, T.J., Reverchon, F., Bai, S.H., Xu, Z., 2019. Nitrogen and carbon cycling associated with litterfall production in monoculture teak and mixed species teak and flueggea stands. *J. Soils Sediments* 19 (4), 1672–1684.
- Vitousek, P.M., Farrington, H., 1997. Nutrient limitation and soil development: experimental test of a biogeochemical theory. *Biogeochemistry* 37, 63e75.
- Vitousek, P., Howarth, R., 1991. Nitrogen limitation on land and in the sea: how can it occur? *Biogeochemistry* 13, 87–115.
- Vitousek, P.M., Porder, S., Houlton, B.Z., Chadwick, O.A., 2010. Terrestrial phosphorus limitation: mechanisms, implications, and nitrogen-phosphorus interactions. *Ecol. Appl.* 20, 5–15.
- Waldrop, M., Firestone, M., 2004. Altered utilization patterns of young and old soil C by microorganisms caused by temperature shifts and N additions. *Biogeochemistry* 67, 235–248.
- Walker, A.P., Beckerman, A.P., Gu, L., Kattge, J., Cernusak, L.A., Domingues, T.F., ... Woodward, F.I., 2014. The relationship of leaf photosynthetic traits – V_{max} and J_{max} – to leaf nitrogen, leaf phosphorus, and specific leaf area: a meta-analysis and modeling study. *Ecol. Evol.* 4 (16), 3218–3235.
- Wang, Y.P., Law, R.M., Pak, B., 2010. A global model of carbon, nitrogen and phosphorus cycles for the terrestrial biosphere. *Biogeosciences* 7 (7), 2261–2282.
- Wang, Y.D., Wang, Z.L., Wang, H.M., Guo, C.C., Bao, W.K., 2012. Rainfall pulse primarily drives litterfall respiration and its contribution to soil respiration in a young exotic pine plantation in subtropical China. *Can. J. For. Res.* 42, 657–666.
- Waring, B.G., Averill, C., Hawkes, C.V., 2013. Differences in fungal and bacterial physiology alter soil carbon and nitrogen cycling: insights from meta-analysis and theoretical models. *Ecol. Lett.* 16, 887–894. <https://doi.org/10.1111/ele.12125>.
- Wen, X., Wang, H., Wang, J., Yu, G., Sun, X., 2010. Ecosystem carbon exchanges of a subtropical evergreen coniferous plantation subjected to seasonal drought, 2003–2007. *Biogeosciences* 7, 357–369.
- Weng, E., Luo, Y., 2011. Relative information contributions of model vs. data to short- and long-term forecasts of forest carbon dynamics. *Ecol. Appl.* 21 (5), 1490–1505.
- Wieder, W.R., Boehnert, J., Bonan, G.B., 2014. Evaluating soil biogeochemistry parameterizations in Earth system models with observations. *Glob. Biogeochem. Cycles* 28, 211–222.
- Wieder, W.R., Cleveland, C.C., Lawrence, D.M., Bonan, G.B., 2015a. Effects of model structural uncertainty on carbon cycle projections: biological nitrogen fixation as a case study. *Environ. Res. Lett.* 10, 044016.
- Wieder, W.R., Cleveland, C.C., Smith, W.K., Todd-Brown, K., 2015b. Future productivity and carbon storage limited by terrestrial nutrient availability. *Nat. Geosci.* 8 (6), 441.
- Wright, I.J., Westoby, M., 2003. Nutrient concentration, resorption and lifespan: leaf traits of Australian sclerophyll species. *Funct. Ecol.* 17 (1), 10–19.
- Wu, X., Luo, Y., Weng, E., White, L., Ma, Y., Zhou, X., 2009. Conditional inversion to estimate parameters from eddy-flux observations. *J. Plant Ecol.* 2 (2), 55–68.
- Xu, T., White, L., Hui, D., Luo, Y., 2006. Probabilistic inversion of a terrestrial ecosystem model: analysis of uncertainty in parameter estimation and model prediction. *Glob. Biogeochem. Cycles* 20 (2).
- Xu, X., Xia, J., Zhou, X., Yan, L., 2020. Experimental evidence for weakened tree nutrient use and resorption efficiencies under severe drought in a subtropical monsoon forest. *J. Plant Ecol.* 13 (5), 649–656.
- Yan, E.-R., Wang, X.-H., Huang, J.-J., 2006. Shifts in plant nutrient use strategies under secondary forest succession. *Plant Soil* 289 (1), 187–197.
- Yan, T., Qu, T., Song, H., Ciais, P., Piao, S., Sun, Z., Zeng, H., 2018. Contrasting effects of N addition on the N and P status of understory vegetation in plantations of sapling and mature *Larix principis-rupprechtii*. *J. Plant Ecol.* 6, 6.
- Zaehele, S., Friend, A.D., 2010. Carbon and nitrogen cycle dynamics in the O-CN land surface model: 1. Model description, site-scale evaluation, and sensitivity to parameter estimates. *Glob. Biogeochem. Cycles* 24, GB1005.
- Zhang, L., 2013. Response of Greenhouse Gas Fluxes to the Addition of Nitrogen and Phosphorus in Subtropical Fir Forest. Master dissertation of Southwest Univ., Chongqing, China.
- Zhang, L., Luo, Y., Yu, G., Zhang, L., 2010. Estimated carbon residence times in three forest ecosystems of eastern China: applications of probabilistic inversion. *J. Geophys. Res.* Biogeosci. 115 (G1).
- Zhang, Q., Xie, J., Lyu, M., Xiong, D., Wang, J., Chen, Y., ... Yang, Y., 2017a. Short-term effects of soil warming and nitrogen addition on the N:P stoichiometry of *Cunninghamia lanceolata* in subtropical regions. *Plant Soil* 411 (1–2), 395–407.
- Zhang, X., Yang, Y., Zhang, C., Niu, S., Yang, H., Yu, G., et al., 2017b. Contrasting responses of phosphatase kinetic parameters to nitrogen and phosphorus additions in forest soils. *Funct. Ecol.* 32 (1), 106–116.
- Zhang, K., Li, M., Su, Y., Yang, R., 2020a. Stoichiometry of leaf carbon, nitrogen, and phosphorus along a geographic, climatic, and soil gradients in temperate desert of Hexi Corridor, northwest China. *J. Plant Ecol.* 3 (1), 114–121. <https://doi.org/10.1093/jpe/rtz045>.
- Zhang, P., Zhou, X., Fu, Y., Shao, J., Zhou, L., Li, S., ... McDowell, N.G., 2020b. Different responses of nonstructural carbohydrates to drought between mature trees and saplings of four species in sub-tropical forests. *For. Ecol. Manag.* 469, 118159.
- Zheng, M., Huang, J., Chen, H., Wang, H., Mo, J., 2015. Responses of soil acid phosphatase and beta-glucosidase to nitrogen and phosphorus addition in two subtropical forests in southern China. *Eur. J. Soil Biol.* 68, 77–84.
- Zheng, Z., Mamuti, M., Liu, H., Shu, Y., Hu, S., Wang, X., Li, B., Lin, L., Li, X., 2017. Effects of nutrient additions on litter decomposition regulated by phosphorus-induced changes in litter chemistry in a subtropical forest, China. *For. Ecol. Manag.* 400, 123–128.
- Zheng, M., Zhou, Z., Luo, Y., Zhao, P., Mo, J., 2019. Global pattern and controls of biological nitrogen fixation under nutrient enrichment: a meta-analysis. *Glob. Chang. Biol.* 25 (6), 1605–1616.
- Zhou, X., Luo, Y., Gao, C., Verburg, P.S.J., Arnone, J.A., Darrouzet-Nardi, A., Schimel, D.S., 2010. Concurrent and lagged impacts of an anomalously warm year on autotrophic and heterotrophic components of soil respiration: a deconvolution analysis. *New Phytol.* 187 (1), 184–198.
- Zhou, G., Zhou, X., Zhang, T., Du, Z., He, Y., Wang, X., Shao, J., Cao, Y., Xue, S., Wang, H., Xu, C., 2017. Biochar increased soil respiration in temperate forests but had no effects in subtropical forests. *For. Ecol. Manag.* 405, 339–349.
- Zhu, J., Wang, Q., He, N., Smith, M.D., Elser, J.J., Du, J., Yuan, G., Yu, G., Yu, Q., 2016. Imbalanced atmospheric nitrogen and phosphorus depositions in China: implications for nutrient limitation. *J. Geophys. Res.* Biogeosci. 121, 1605–1616.
- Zhu, Q., Riley, W.J., Tang, J., Collier, N., Hoffman, F.M., Yang, X., Bisht, G., 2019. Representing nitrogen, phosphorus, and carbon interactions in the E3SM Land Model: development and global benchmarking. *J. Adv. Model. Earth Syst.* 121 (6), 1605–1616.